

Toward the Synthetic Control of the HOMO–LUMO Gap in Binuclear Systems: Insights from Density Functional Calculations

Alvaro Muñoz-Castro,[†] Desmond Mac-Leod Carey,[†] Cesar Morales-Verdejo,[‡] Ivonne Chávez,[‡] Juan Manuel Manríquez,[‡] and Ramiro Arratia-Pérez^{*†}

[†]Departamento de Ciencias Químicas, Universidad Andres Bello, Republica 275, Santiago, Chile, and

[‡]Departamento de Química Inorgánica, Facultad de Química, Pontificia Universidad Católica de Chile, Casilla 306, Santiago, Chile

Received November 24, 2009

Computational methods based on density functional theory have been applied to address the design of tailored HOMO–LUMO gap bimetallic complexes. We focus our attention on the $[\text{Cp}^*\text{Fe}-(\text{L})-\text{FeCp}^*]$ system, where two ferrocenyl units are linked through the dianion of fused ring ligands such as pentalene, *s*-indacene, dicyclopenta- $[b,g]$ -naphthalene, dicyclopenta- $[b,l]$ -anthracene and dicyclopenta- $[b,l]$ -tetracene. Our DFT calculations on the title organometallic complexes suggest a controlled decrease in the HOMO–LUMO gap, which is desirable for studies on electron-transfer phenomena, as well as the design potential devices for molecular electronic purposes.

Introduction

Intramolecular interaction between redox centers mediated by linking ligands is a relevant process in chemical and biological systems,¹ where the electron-transfer process plays a key role ranging from simple redox reactions to more complex enzymatic cycles. Since the publication of the mixed valence (MV) Creutz-Taube ion $[(\text{NH}_3)_5\text{Ru}(\mu\text{-pyz})\text{Ru}(\text{NH}_3)_5]^{5+}$, pyz = pyrazine) in the late 1960s,² major efforts have been pursued for the development and understanding of other MV systems,^{3,4} due to their unusual spectroscopical

properties⁵ and their potential application in molecular electronics⁶ and catalysis.⁷

The formation of MV states between different redox sites is an intriguing capability of polynuclear metallic complexes, particularly those with ferrocenyl fragments which are characterized by electronic delocalization between metal centers.^{8,9} The geometry of the linking ligand certainly determines the behavior of the electronic communication;⁹ e.g., the MV bimetallic complexes $[\text{Cp}^*\text{Fe}-\textit{as}\text{-indacenediide}-\text{FeCp}^*]^+\text{BF}_4^-$, $[\text{Cp}^*\text{Fe}-\text{dicyclopenta-}[a,f]\text{-naphthalenediide}-\text{FeCp}^*]^+\text{BF}_4^-$,¹⁰ and $[\text{Cp}^*\text{Fe}-\text{dicyclopenta-}[a,h]\text{-anthracenediide}-\text{FeCp}^*]^+\text{BF}_4^-$ ¹¹ can be considered class II in the Robin–Day

*To whom correspondence should be addressed. E-mail: rarratia@unab.cl (R. A.-P.).

(1) (a) Lin, J. P.; Balabin, I. A.; Beratan, D. N. *Science* **2005**, *310*, 1311. (b) Creutz, C. *Prog. Inorg. Chem.* **1983**, *30*, 1. (c) Chen, P.; Meyer, T. J. *Chem. Rev.* **1998**, *98*, 1439. (d) Holm, R. H.; Kennepohl, P.; Solomon, E. I. *Chem. Rev.* **1996**, *96*, 2239. (e) Demadis, K. D.; Hartshorn, C. M.; Meyer, T. J. *Chem. Rev.* **2001**, *101*, 2655. (f) Lau, V. C.; Berben, L. A.; Long, J. R. *J. Am. Chem. Soc.* **2002**, *124*, 9042. (g) Ward, M. D. *Chem. Soc. Rev.* **1995**, *24*, 121.

(2) (a) Creutz, C.; Taube, H. *J. Am. Chem. Soc.* **1973**, *95*, 1086. (b) Demadis, K. D.; Hartshorn, C. M.; Meyer, T. J. *Chem. Rev.* **2001**, *101*, 2655.

(3) (a) Astruc, D. *Electron Transfer and Radical Processes in Transition-Metal Chemistry*; Wiley-VCH: New York, 1995. (b) Prassides, K. *Mixed-Valency Systems: Applications in Chemistry, Physics and Biology*; Kluwer Academic Publishers: Dordrecht, The Netherlands, 1991. (c) Balzani, V.; Credi, A.; Venturi, M. *Molecular Devices and Machines: Concepts and Perspectives for the Nanoworld*; Wiley-VCH: New York, 2008.

(4) (a) Astruc, D. *Acc. Chem. Res.* **1997**, *30*, 383. (b) Rocha, R.; Rein, F. N.; Shreve, A. P.; Concepcion, J. J.; Meyer, T. J. *Angew. Chem., Int. Ed.* **2008**, *47*, 503.

(5) (a) Hush, N. S. *Coord. Chem. Rev.* **1985**, *64*, 135. (b) Blondin, G.; Girerd, J.-J. *Chem. Rev.* **1990**, *90*, 1359.

(6) (a) Launay, J.-P. *Chem. Soc. Rev.* **2001**, *30*, 386. (b) Basch, H.; Ratner, M. A. *J. Chem. Phys.* **2005**, *123*, 234704. (c) Manners, I. *Adv. Organomet. Chem.* **1995**, *37*, 131. (d) D'Alessandro, D. M.; Keene, F. R. *Chem. Rev.* **2006**, *106*, 2270.

(7) (a) Esponda, E.; Adams, C.; Burgos, F.; Chávez, I.; Manríquez, J. M.; Delpéch, F.; Castel, A.; Gornitzka, H.; Riviere-Baudet, M.; Riviere, P. *J. Organomet. Chem.* **2006**, *691*, 3011. (b) Adams, C.; Morales-Verdejo, C.; Morales, V.; MacLeod-Carey, D.; Manríquez, J. M.; Chávez, I.; Muñoz-Castro, A.; Delpéch, F.; Castel, A.; Gornitzka, H.; Riviere-Baudet, M.; Riviere, P.; Molins, E. *Eur. J. Inorg. Chem.* **2009**, *6*, 784. (c) Cecon, A.; Santi, S.; Orian, L.; Bisello, A. *Coord. Chem. Rev.* **2004**, *248*, 683.

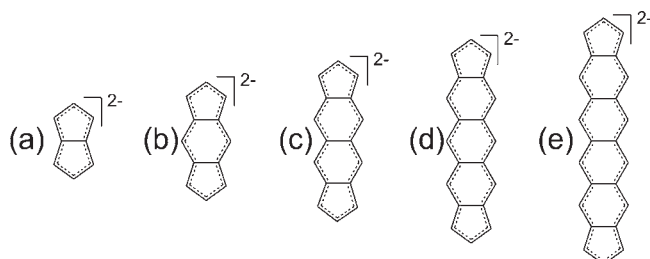
(8) (a) Manríquez, J. M.; Ward, M. D.; Reiff, W. M.; Calabrese, J. C.; Jones, N. L.; Carroll, P. J.; Bunel, E. E.; Miller, J. S. *J. Am. Chem. Soc.* **1995**, *117*, 6182. (b) Mac-Leod Carey, D.; Morales-Verdejo, C.; Muñoz-Castro, A.; Burgos, F.; Abril, D.; Adams, C.; Molins, E.; Chávez, I.; Manríquez, J. M. *Polyhedron* **2010**, *29*, 1137.

(9) (a) Bunel, E. E.; Valle, L.; Jones, N. L.; Carroll, P. J.; Barra, C.; Gonzalez, M.; Muñoz, N.; Visconti, G.; Aizman, A.; Manríquez, J. M. *J. Am. Chem. Soc.* **1988**, *110*, 6596. (b) Barlow, S. *Inorg. Chem.* **2001**, *40*, 7047. (c) Barlow, S.; O'Hare, D. *Chem. Rev.* **1997**, *97*, 637. (d) Rulkens, R.; Lough, A. J.; Manners, I.; Lovelace, S. R.; Grant, C.; Geiger, W. E. *J. Am. Chem. Soc.* **1996**, *118*, 12683.

(10) Alfonso, G.; Chávez, I.; Arancibia, V.; Manríquez, J. M.; Garland, M. T.; Roig, A.; Molins, E.; Fortunato Baggio, R. *J. Organomet. Chem.* **2001**, *620*, 32.

(11) Amshumali, M. K.; Chávez, I.; Arancibia, V.; Burgos, F.; Manríquez, J. M.; Molins, E.; Roig, A. *J. Organomet. Chem.* **2005**, *690*, 1340.

Scheme 1. Fused Delocalized Polycyclic Arenes



framework,¹² which means a localized valence system. On the other hand, the MV bimetallic complexes $[\text{Cp}^*\text{Fe}(\text{pentalenediide})\text{FeCp}^*]^+\text{BF}_4^-$ ^{8,9} and $[\text{Cp}^*\text{Fe}(s\text{-indacenediide})\text{FeCp}^*]^+\text{BF}_4^-$ ^{8,9} are fully delocalized and considered class III systems. Hence, fused delocalized polycyclic acene ligands, such as pentalenediide and *s*-indacenediide, are particularly effective for promoting the interaction between different metallic redox sites due to their geometry, rigidity, and electron-rich π system.^{8,9}

In recent years, molecules that possess a small highest occupied–lowest unoccupied molecular orbital (HOMO–LUMO) gap¹³ have demonstrated a variety of unusual optoelectronic properties^{14a} and multielectron-transfer behaviors,^{14b} making them attractive targets for studying electron-transfer phenomena, as well as molecular electronics applications.¹⁵ This fact has prompted us to investigate synthetic approaches for the design of small HOMO–LUMO gap organometallic systems containing two redox centers in their structure. Thus, in order to achieve a better understanding of the variation of the electronic structure in relation to the length of the linearly annelated linking ligand over the electronic communication and the HOMO–LUMO gap, DFT calculations have been done for systems of the type $[\text{Cp}^*\text{Fe}(\text{L})\text{FeCp}^*]$, in which two permethylated-ferrocenyl fragments ($[(\text{Cp}^*\text{Fe}\cdots\text{FeCp}^*)^{2+}]$) are linked by an L^{2-} ligand such as pentalenediide (**a**, see Scheme 1), *s*-indacenediide (**b**), dicyclopenta-*[b,g]*-naphthalenediide (**c**), dicyclopenta-*[b,i]*-anthracenediide (**d**), and dicyclopenta-*[b,l]*-tetracenediide (**e**), which can be considered as the insertion of *n* benzoid (Bz) moieties between two fused cyclopentadiene rings,¹⁶ where *n* = 0, 1, 2, 3 and 4, affording a 10, 14, 18, 22, and 26 πe^- conjugated ligands, respectively.

Computational Details

The relativistic density functional theory calculations were carried out employing the ADF2008.01 code,¹⁷ incorporating scalar corrections via the two-component ZORA

Hamiltonian.^{18a,b} Geometry optimizations were done under C_{2h} geometry restraints and, in addition, without any symmetry restraint for comparison, via the analytical energy gradient method implemented by Verluis and Ziegler,^{18c} employing the triple- ζ Slater basis set plus a polarization function (STO-TZP) in conjunction with the general gradient approximation (GGA) as well as Becke's three parameter hybrid functional with the Lee–Yang–Parr correlation functional B3LYP (see Supporting Information for details). Several GGA exchange-correlation functionals have been tested showing similar results to those obtained with TZP/BP86 calculations; thus in the following, we focus our analysis on the geometrical results provided by TZP/BP86 calculations.

In the paramagnetic counterparts, the presence of symmetry elements forces the complete electron delocalization between the metal centers, due to the fact that these centers are considered equal by the C_2 operation of symmetry within the unrestricted DFT formalism. Therefore, to describe correctly the metal–metal interaction, it is necessary to treat the metal atoms as distinct redox centers that behave independently in both geometry and electronic calculations. This had been achieved through the use of the broken-symmetry method (BS),¹⁹ developed by Noodleman and co-workers, where some or all symmetry elements are not considered in the calculations.

Results and Discussion

The neutral $[(\text{Cp}^*\text{Fe})_2(\mathbf{a})]^{0a}$ (**1**) and $[(\text{Cp}^*\text{Fe})_2(\mathbf{b})]^{0b}$ (**2**) and the hypothetical (not yet synthesized) $[(\text{Cp}^*\text{Fe})_2(\mathbf{c})]^{0c}$ (**3**), $[(\text{Cp}^*\text{Fe})_2(\mathbf{d})]^{0d}$ (**4**), and $[(\text{Cp}^*\text{Fe})_2(\mathbf{e})]^{0e}$ (**5**) were studied under C_{2h} geometry restraints, in order to rationalize the results employing the highest symmetry available for these systems. However, the C_{2h} results do not differ from those obtained with C_1 , without any symmetry restraints. The geometries of **1** and **2** are in reasonable agreement with the experimental data from refs 8 and 9a (see Table 1).

For the monocationic (paramagnetic) mixed-valence counterparts (**1**⁺, **2**⁺, **3**⁺, **4**⁺, and **5**⁺), broken symmetry (BS)¹⁹ geometry optimizations have been done within the unrestricted DFT formalism, with a modified unsymmetrical starting geometry as well as a starting potential that initially localizes the unpaired electron on one redox center, neglecting any symmetry operations (i.e., no symmetry statement), in order to treat each ferrocenyl fragment as a distinct center that behaves independently. In all cases, the final self-consistent (SCF) procedure exhibits a full delocalized paramagnetic system, with the unpaired electron in the same proportion on both metallic moieties (see the spin-density in Figure 2).

The HOMO–LUMO gap values for **1**, **2**, **3**, **4**, and **5** were estimated employing two DFT methods for comparison,²³ the general gradient approximation (GGA) and Becke's three-parameter hybrid functional with the Lee–Yang–Parr correlation functional (B3LYP). Several GGA exchange-correlation functionals have been tested (Supporting Information)

(12) Robin, M. B.; Day, P. *Adv. Inorg. Chem. Radiochem.* **1967**, *10*, 247.

(13) (a) Metzger, R. M. *Acc. Chem. Res.* **1999**, *32*, 950. (b) Perepichka, D. F.; Bryce, M. R. *Angew. Chem., Int. Ed.* **2005**, *44*, 5370.

(14) (a) Roncali, J. *Chem. Rev.* **1997**, *97*, 173. (b) Kobayashi, A.; Fujiwara, E.; Kobayashi, H. *Chem. Rev.* **2004**, *104*, 5243.

(15) (a) Sonmez, G.; Meng, H.; Wudl, F. *Chem. Mater.* **2003**, *15*, 4923.

(b) Carroll, R. L.; Gorman, C. B. *Angew. Chem., Int. Ed.* **2002**, *41*, 4378.

(16) Garcia Cuesta, I.; Coriani, S.; Lazzeretti, P.; Sanchez de Meras, A. M. *J. ChemPhysChem* **2006**, *7*, 240.

(17) te Velde, G.; Bickelhaupt, F. M.; Van Gisbergen, S. J. A.; Guerra, C. F.; Baerends, W. J.; Snijders, J. G.; Ziegler, T. *J. Comput. Chem.* **2001**, *22*, 931. *ADF2008.01*; SCM, Theoretical Chemistry, Vrije Universiteit: Amsterdam, The Netherlands.

(18) (a) Van Lenthe, E.; Baerends, E. J.; Snijders, J. G. *J. Chem. Phys.* **1994**, *101*, 9783. (b) Te Velde, G.; Bickelhaupt, F. M.; Van Gisbergen, S. J. A.; Fonseca Guerra, C.; Baerends, E. J.; Snijders, J. G.; Ziegler, T. *J. Comput. Chem.* **2001**, *22*, 931. (c) Verluis, L.; Ziegler, T. *J. Chem. Phys.* **1988**, *88*, 322.

(19) (a) Noodleman, L.; Norman, J. G., Jr. *J. Chem. Phys.* **1979**, *70*, 4903.

(b) Noodleman, L. *J. Chem. Phys.* **1981**, *74*, 5737. (c) Ziegler, T. *Chem. Rev.* **1991**, *91*, 651.

(20) Calculated as $[(C3 - M) - (C1 - M)] / (C1 - M) \%$. For further details, see: Muñoz-Castro, A.; Mac-Leod Carey, D.; Arratia-Pérez, R. *Polyhedron* **2009**, *28*, 1561.

(21) (a) Morokuma, K. *J. Chem. Phys.* **1971**, *55*, 1236. (b) Ziegler, T.; Rauk, A. *Theor. Chim. Acta* **1977**, *46*, 1. (c) Bickelhaupt, F. M.; Baerends, E. J. In *Reviews in Computational Chemistry*; Lipkowitz, K. B., Boyd, D. B., Eds.; Wiley-VCH: New York, 2000; Vol. 15, p 1.

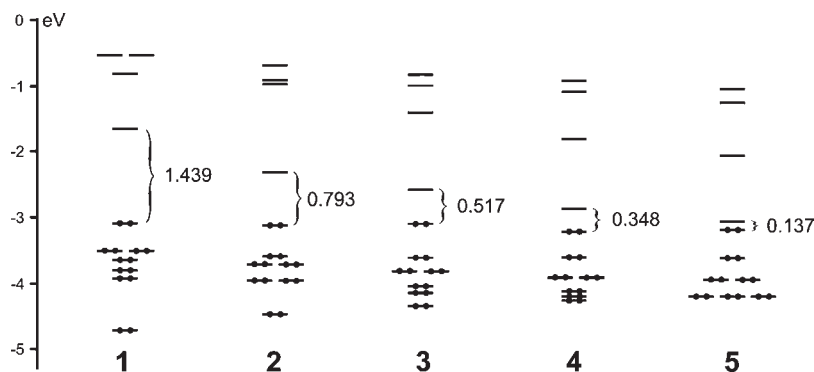
(22) Lee, C.; Yang, W.; Parr, R. G. *Phys. Rev. B* **1988**, *37*, 785.

(23) For a recent discussion about how the level of theory affects the eigenvalues of the frontier orbitals, see: Zhang, G.; Musgrave, C. B. *J. Phys. Chem. A* **2007**, *111*, 1554.

Table 1. Selected Geometrical Parameters, the HOMO–LUMO Gap (H–L Gap, eV), and the Energy Decomposition Analysis (EDA) in kcal/mol of the Bonding Energy of the $(\text{Cp}^*\text{Fe})_2^{2+}$ –(linking ligand) $^{2-}$ Interaction for **1**, **2**, **3**, **4** and **5**^a

		1	2	3	4	5
Fe–C ₅ ^b	calcd ^c	1.694 (7%)	1.703 (6%)	1.683 (4%)	1.710 (7%)	1.672 (1%)
	exp.	1.640 (5%) ^e	1.731 (5%) ^f			
H–L gap	GGA ^c	1.439	0.793	0.517	0.348	0.137
	hyb. ^d	3.804	2.553	1.932	1.605	1.220
$\Delta E_{\text{Pauli}}^g$		336.0	328.7	339.5	322.9	348.7
$\Delta V_{\text{elstat}}^g$		–404.2	–386.6	–383.4	–369.1	–348.8
ΔE_{orb}^g		–328.8	–320.4	–327.1	–319.8	–355.7
ΔE_{int}^g		–397.0	–378.3	–371.1	–365.9	–355.8

^a In addition, selected geometrical parameters for **1**⁺, **2**⁺, **3**⁺, **4**⁺, and **5**⁺. ^b Distance between the Cp*Fe⁺ moiety and the centroid located in the middle of the cyclopentadienyl ring (C₅) of the bridging ligand. Percent deviations from the η^5 hapticity are given between parentheses.²⁰ ^c From a TZP/BP86 calculation. ^d From a TZP/B3LYP calculation. ^e From ref 9a. ^f From ref 8. ^g Bonding energy or the interaction energy between the $[(\text{Cp}^*\text{Fe})_2]^{2+}$ and $[\text{L}^{2-}]$ fragments, $\Delta E_{\text{int}} = \Delta V_{\text{elstat}} + \Delta E_{\text{Pauli}} + \Delta E_{\text{orb}}$,²¹ from a TZP/BP86 calculations.

**Figure 1.** Frontier energy levels of **1**, **2**, **3**, and **4**, denoting the HOMO–LUMO gap as suggested from TZP/BP86 calculations.

showing similar results to those obtained with TZP/BP86 calculations; thus in the following, we focus our analysis on the results provided by TZP/BP86 calculations. Note that the B3LYP HOMO–LUMO gap values are larger than the obtained via GGA, due to the 20% exact Hartree–Fock exchange,²³ but clearly reproduce the trend suggested by the GGA calculations (Table 1).

The calculated geometries (Table 1) of **1**, **2**, **3**, **4**, and **5** suggest that the $(\text{Cp}^*\text{Fe})^+$ fragment is bound in an almost η^5 coordination mode to the five-member rings of the bridging ligand with deviations from 7% for **1** to 1% for **5**.²⁰ The metal five-member ring distance decrease for **1**, **3**, and **5** (i.e., the even number of Bz moieties), from 1.694 to 1.672 Å, and increase for **2** and **4**, from 1.703 to 1.710 Å.

In order to achieve a better understanding in the $[(\text{Cp}^*\text{Fe})_2]^{2+}$ – $[\text{L}^{2-}]$ ($\text{L}^{2-} = \mathbf{a}, \mathbf{b}, \mathbf{c}, \mathbf{d},$ and \mathbf{e}) interaction, energy decomposition analysis (EDA) via the Morokuma–Ziegler scheme²¹ (Table 1) was carried out for the interaction energy between the $[(\text{Cp}^*\text{Fe})_2]^{2+}$ and $[\text{L}^{2-}]$ fragments, defined by eq 1:

$$\Delta E_{\text{int}} = \Delta E_{\text{tot}} - \Delta E([(Cp^*Fe)_2]^{2+}) - \Delta E([L^{2-}]) \quad (1)$$

where ΔE_{tot} refers to the total bonding energy of the complex (or the negative of the atomization energy), and $\Delta E([(Cp^*Fe)_2]^{2+})$ and $\Delta E([L^{2-}])$ refer to the bonding energy of each isolated fragment at the geometry that they acquire in the overall complex. The bonding energy is calculated to be the difference between the energy of the molecule and that of their constituent atoms. In this scheme, ΔE_{int} can be further decomposed in three terms (eq 2), where ΔV_{elstat} accounts for the electrostatic interaction, ΔE_{Pauli} gives the electronic repulsion due to the Pauli principle, and ΔE_{orb} accounts for

the stabilizing orbital interaction term.²¹

$$\Delta E_{\text{int}} = \Delta V_{\text{elstat}} + \Delta E_{\text{Pauli}} + \Delta E_{\text{orb}} \quad (2)$$

In this sense, the calculations suggest that the increase of the orbital stabilization term (ΔE_{orb}) into the total stabilization energy account for the decrease of the bond lengths for **1**, **3**, and **5**. In contrast, for odd numbers of Bz moieties (i.e., for **2** and **4**), this term induces a slight increase in the bond length. Moreover, the interaction energy decreases from –397.0 kcal/mol for **1** to –355.8 for **5**. The total interaction energy (ΔE_{int}) shows a slightly electrostatic character (~55% of the total energy) compared to the orbital character and decreases from **1** to **5** due to the increase in the ligand character in the bonding orbitals of the metal-bridging ligand interaction.

In Figure 1, the TZP/BP86 frontier MO diagram is presented showing the mainly metallic block of the electronic structure. The decreasing of the HOMO–LUMO gap from **1** to **5** (Figure 1 and Table 1) must be noted. Particularly **3**, **4**, and **5** present small values for the HOMO–LUMO gap, which are promising for designing systems which can act as unimolecular rectifiers.^{13–15} In addition, the isoelectronic $[(\text{Cp}^*\text{Fe})\text{L}(\text{CoCp}^*)]^+$ (note the asymmetry in the redox centers) is envisioned to act as a potential donor–acceptor rectifier (one-way conductor)¹³ due to the fact that the HOMO is centered on the Fe(II) site and the LUMO is centered on the Co(III) site, with a reversible redox behavior (see the pentalenediide case from ref 8).

Thus, both GGA and hybrid DFT calculations suggest that the increase of the benzoid rings between the cyclopentadienyl groups is a plausible synthetic strategy to design binuclear systems with controlled small HOMO–LUMO gaps (Table 1). Moreover, the increase of the linking ligand

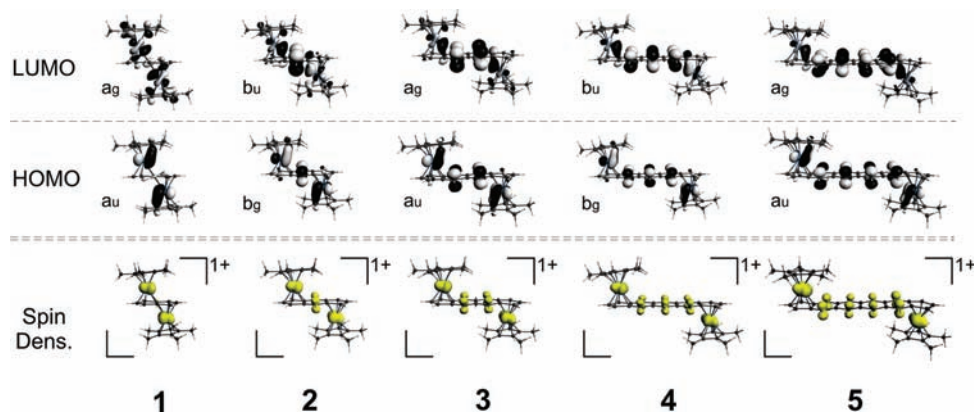


Figure 2. Selected frontier orbital plots (isosurface value at 0.03 au) of the neutral complexes and spin densities of the monocationic counterparts (isosurface value at 0.3 au), obtained from broken symmetry (BS) calculations.

contribution to the HOMO and LUMO (Supporting Information) from 4% to 51% and from 10% to 80%, respectively (Figure 2), suggests that the synthetic manipulation of the bridging ligand certainly varies the energy of the energy levels (eigenvalues) and is suggested for a fine tailoring of the HOMO–LUMO gap. Several attempts to increase the benzoid rings between the cyclopentadienyl groups have been reported; see for example the synthesis of $[\text{Cp}^*\text{Fe}(\text{dicyclopenta-}[a,f]\text{-naphthalenediide})\text{FeCp}^*]^+\text{BF}_4^-$ ¹⁰ and $[\text{Cp}^*\text{Fe}(\text{dicyclopenta-}[a,h]\text{-anthracenediide})\text{FeCp}^*]^+\text{BF}_4^-$ ¹¹.

For the mixed valence states (i.e., 1^+ , 2^+ , 3^+ , 4^+ , and 5^+) of the title compounds, the spin-density suggests that these systems may behave as class III systems, with an equal amount of the unpaired electron in both metallic redox centers (Figure 2) increasing the bridging ligand participation from 4% to 60% from 1^+ to 5^+ , respectively. In agreement with the experimental findings for 1^+ and 2^+ ,⁸ this allows one to consider them as class III systems. Thus, it is suggested that the hypothetical 3^+ , 4^+ , and 5^+ should exhibit similar behavior to that of 1^+ and 2^+ . However, it is possible that 3^+ , 4^+ , and 5^+ behave as class II systems in solution, due to the increased distance between the redox centers.

Conclusion

Our calculations suggest that increasing the length of the bridging ligand in the studied complexes is a plausible

synthetic strategy to achieve a controlled HOMO–LUMO gap in bimetallic systems for studies on electron-transfer phenomena and molecular electronic purposes. In the mixed valence states (paramagnetic systems), broken symmetry (BS) calculations suggest a complete delocalization of the unpaired electron through the whole system that leads to an equal amount of spin density on both metallic redox centers, as well as an increasing participation of the bridging ligand (L^{2-}) as a function of its length. In addition, the calculations suggest that the proposed systems **3**, **4**, and **5** are interesting to synthesize due to their predicted small HOMO–LUMO gap, which leads to the onset of a conduction band.

Acknowledgment. The authors thank the reviewers for their useful comments. This work has been supported by UNAB-DI-09-09/I; Conicyt Fellowship 21100513; MECESUP FSM 0605; FONDECYT Grants 1070345, 1060589, and 1100283; UNAB-DI-02-09/R; PROJECT MILLENNIUM No. P07-006-F; and apoyo de tesis doctoral 24080034 Conicyt.

Supporting Information Available: HOMO–LUMO gap obtained using several exchange correlation functionals, percent composition of HOMO and LUMO, and spin density analysis. This material is available free of charge via the Internet at <http://pubs.acs.org>.